LETTERS
PUBLISHED ONLINE: 7 JULY 2013 | DOI: 10.1038/NPHOTON.2013.156
nature photonics

Compact high-repetition-rate source of coherent 100 eV radiation

I. Pupeza[1,2†*], S. Holzberger[1,2†], T. Eidam[3], H. Carstens[1,2], D. Esser[4], J. Weitenberg[5], P. Rußbüldt[4], J. Rauschenberger[1,2], J. Limpert[3], Th. Udem[1], A. Tünnermann[3], T. W. Hänsch[1,2], A. Apolonski[1,2], F. Krausz[1,2] and E. Fill[1,2]

Coherently enhancing laser pulses in a passive cavity provides ideal conditions for high-order harmonic generation in a gas, with repetition rates around 100 MHz (refs 1–3). Recently, extreme-ultraviolet radiation with photon energies of up to 30 eV was obtained, which is sufficiently bright for direct frequency-comb spectroscopy at 20 eV (ref. 4). Here, we identify a route to scaling these radiation sources to higher photon energies. We demonstrate that the ionization-limited attainable intracavity peak intensity increases with decreasing pulse duration. By enhancing nonlinearly compressed pulses of an Yb-based laser and coupling out the harmonics through a pierced cavity mirror, we generate spatially coherent 108 eV (11.45 nm) radiation at 78 MHz. Exploiting the full potential of the demonstrated techniques will afford high-photon-flux ultrashort-pulsed extreme-ultraviolet sources for a number of applications in science and technology, including photoelectron spectroscopy, coincidence spectroscopy with femtosecond to attosecond resolution[5,6] and characterization of components and materials for nanolithography[7].

Over the past two decades, extreme-ultraviolet (XUV) pulses obtained via laser-driven high-harmonic generation (HHG) have offered new insights into ultrafast processes in atoms, molecules and solids[8–10]. For this field to progress, it is essential that table-top sources of coherent, broadband, high-power XUV radiation continue to develop; indeed, this remains an ongoing challenge. Pump–probe techniques, in particular, would benefit from higher repetition rates[11–13] because of the consequent improvement in statistics, the mitigation of space-charge effects and the achievement of shorter acquisition times. Photoelectron spectroscopy[5], photoelectron emission microscopy[14,15], coincidence spectroscopy (relying on correlated detection of charged particles)[16,17] and XUV frequency-comb spectroscopy[4] could all advance dramatically with powerful megahertz XUV sources.

To meet this demand, the technique of coherently stacking ultrashort pulses of a mode-locked laser in a passive multi-megahertz repetition-rate enhancement cavity housing the HHG process seems to be most promising. The low losses experienced by the intracavity pulse with each pass through the gas target enable a large power enhancement[1–3], leading to pulse energies typically obtained only with laser amplifiers operating at repetition rates well below 1 MHz (refs 8–10). The viability of this technology was recently corroborated by record average powers for table-top coherent sources at photon energies up to 30 eV (refs 4,11,18,19). However, the previously reported enhancement cavities have several major limitations. First, the maximum attainable peak intensity has so far been limited either by the available average power from laser systems emitting pulses of a few tens of femtoseconds[1] or by ionization-related effects observed with lasers providing higher average powers at the expense of increased pulse durations (typically around 100 fs)[18,20,21]. This intensity limitation precludes scaling the generated XUV photon energies. Moreover, the output coupling of the collinearly generated XUV beam is based on reflection[1,2,19] or diffraction[4,11,18]. Reflection-based output couplers imply the use of an intracavity beamsplitter, which introduces limitations such as nonlinearities, a limited bandwidth or polarization discrimination. Diffraction-based output couplers are well suited for applications requiring the angular dispersion of the XUV spectrum[4]. However, this constitutes a disadvantage for several spectroscopy schemes, such as time-resolved pump–probe experiments.

In this work we present an apparatus that overcomes these limitations. First, we investigate the dependence of the ionization-induced peak power enhancement limitation[18,20,21] on pulse duration. In single-pass HHG experiments it has long been known that the XUV yield for high photon energies increases with decreasing pulse duration, but here we find that short pulse durations also mitigate this ionization-related enhancement limitation, allowing for higher intracavity peak intensities. Therefore, decreasing the pulse duration in cavity-assisted HHG systems is essential for increasing the generated photon energies. To reduce the pulse duration while maintaining high average powers, for the first time we nonlinearly enhance compressed femtosecond pulses from an Yb-based fibre laser. Moreover, output coupling is realized through an on-axis opening in a cavity mirror[22], experimentally demonstrating the first broadband output coupler whose efficiency increases with photon energy.

The set-up (Fig. 1) consists of an Yb-doped crystal-based 78 MHz oscillator with a central wavelength of 1,040 nm, a chirped-pulse fibre amplifier boosting the average power to 60 W, a nonlinear pulse compression stage[23] and an enhancement cavity in the form of a ring resonator[24]. The full-width at half-maximum (FWHM) of the intensity autocorrelation of the amplified pulses is 267 fs. This implies a pulse duration of 172 fs by assuming a sech^2-temporal profile. The pulses are spectrally broadened via self-phase modulation in a large-mode-area fibre and temporally compressed with a set of chirped multilayer mirrors. To avoid damage by self-focusing in the spectral broadening fibre, circular polarization is used for compression[25]. To prevent spectral filtering by the passive cavity, we limit the broadening to 60 nm (full width at −10 dB) by appropriate choice of the fibre length. This corresponds

[1]Max-Planck-Institut für Quantenoptik, Hans-Kopfermann-Strasse 1, 85748 Garching, Germany, [2]Ludwig-Maximilians-Universität München, Fakultät für Physik, Am Coulombwall 1, 85748 Garching, Germany, [3]Friedrich-Schiller-Universität Jena, Institut für Angewandte Physik, Albert-Einstein-Strasse 15, 07745 Jena, Germany, [4]Fraunhofer-Institut für Lasertechnik, Steinbachstrasse 15, 52074 Aachen, Germany, [5]RWTH Aachen University, Lehrstuhl für Lasertechnik, Steinbachstrasse 15, 52074 Aachen, Germany; †These authors contributed equally to this work. *e-mail: ioachim.pupeza@mpq.mpg.de

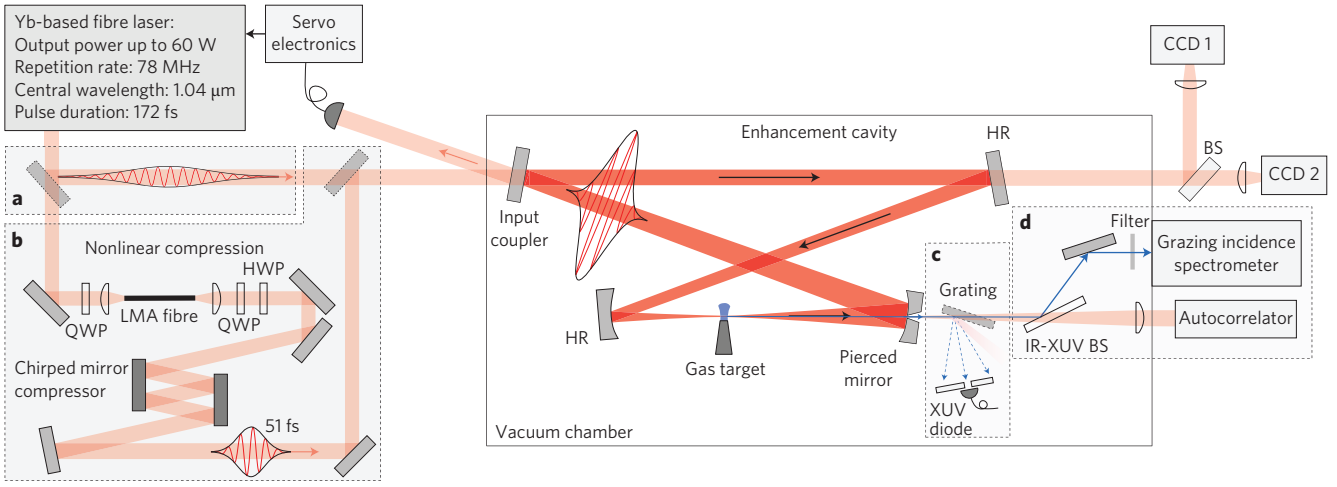

Figure 1 | Experimental set-up for intracavity HHG. a–d, Amplified laser pulses are coherently stacked inside a passive resonator. The pulses can either be enhanced directly after the chirped-pulse amplifier (**a**) or first compressed nonlinearly (**b**). QWP, quarter-wave plate; HWP, half-wave plate; LMA, large-mode-area fibre. The harmonic radiation generated in the cavity focus is coupled out through a hole in the subsequent mirror (clear aperture radius typically ~40 μm). The coherent build-up inside the cavity is maintained with a Pound–Drever–Hall locking scheme[30]. CCD cameras image the transverse intensity distribution of the fundamental mode at each of the two curved mirrors. BS, beam splitter; HR, high reflector. The output coupled XUV radiation is either dispersed with a grating, for measuring the average power in individual harmonics with an XUV photodiode (**c**) or sent to a grazing incidence spectrometer, equipped with an XUV CCD camera (**d**).

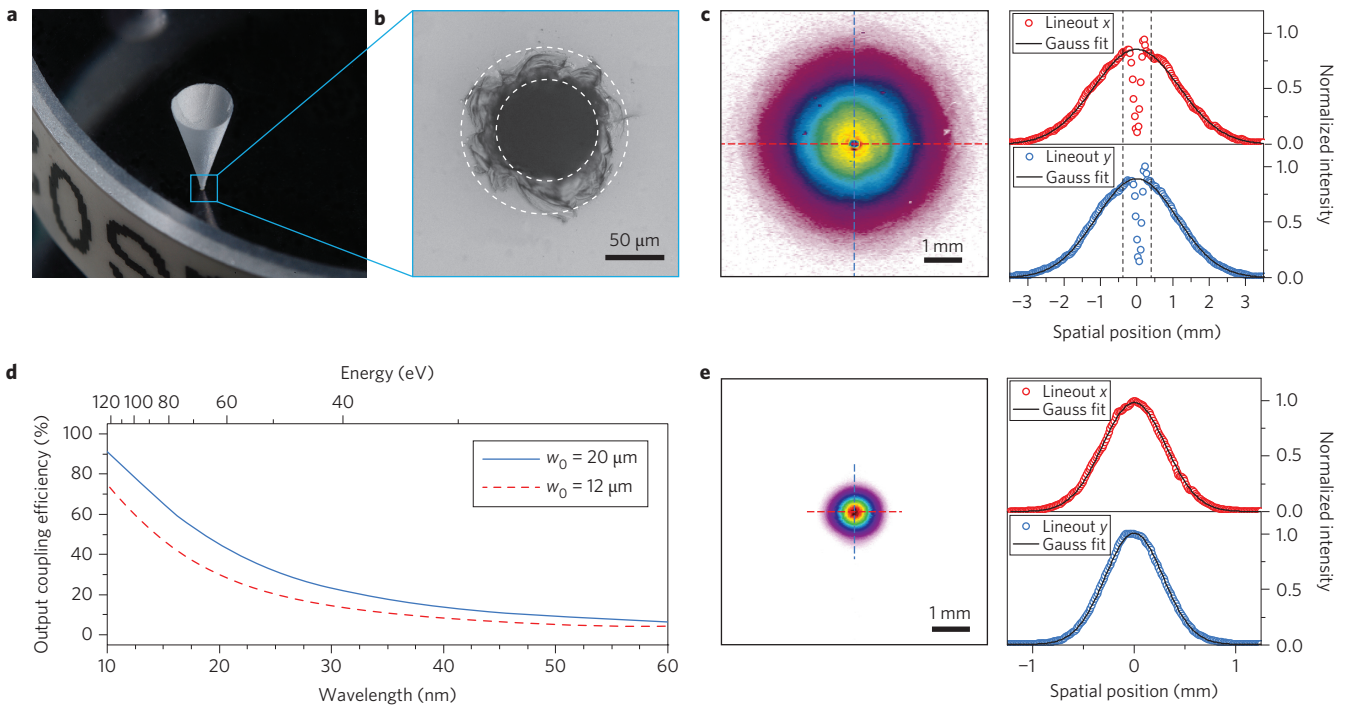

Figure 2 | XUV output coupling mirror, fundamental beam profiles and calculated output coupling efficiency. a, Photograph of the XUV output coupler, showing the back side of the pierced mirror. **b**, Close-up of the opening in the mirror surface reveals chipping at the edges. The outer hole radius ($r_h \approx 80$ μm) determines the roundtrip losses for the fundamental mode. The inner radius (that is, the clear aperture radius) of ~40 μm determines the output coupling efficiency for the harmonics. **c**, Fundamental beam intensity profile at the position of the output coupler (for $w_0 = 12$ μm) and lineouts with Gaussian fits. The fits were performed by excluding the region of the hole (indicated by the dashed lines). **d**, Estimated output coupling efficiency for the two implemented focusing geometries (see Methods). **e**, Fundamental beam intensity profile at the mirror before the focus (for $w_0 = 12$ μm) and lineouts with excellent Gaussian fits.

to 51 fs pulses with an average power of 43 W. It should be emphasized that cavity mirrors supporting a broader spectrum can be designed, in principle[1].

The intracavity generated XUV radiation emerges at a much smaller divergence angle than the fundamental beam and is coupled out through a small hole in the mirror behind the focus (Fig. 2a–c). This method offers the following advantages: the harmonics leave the cavity collinearly; none of the harmonic and fundamental pulse parameters (bandwidth, spectral phase) is affected; and the output coupling efficiency tends to increase with photon

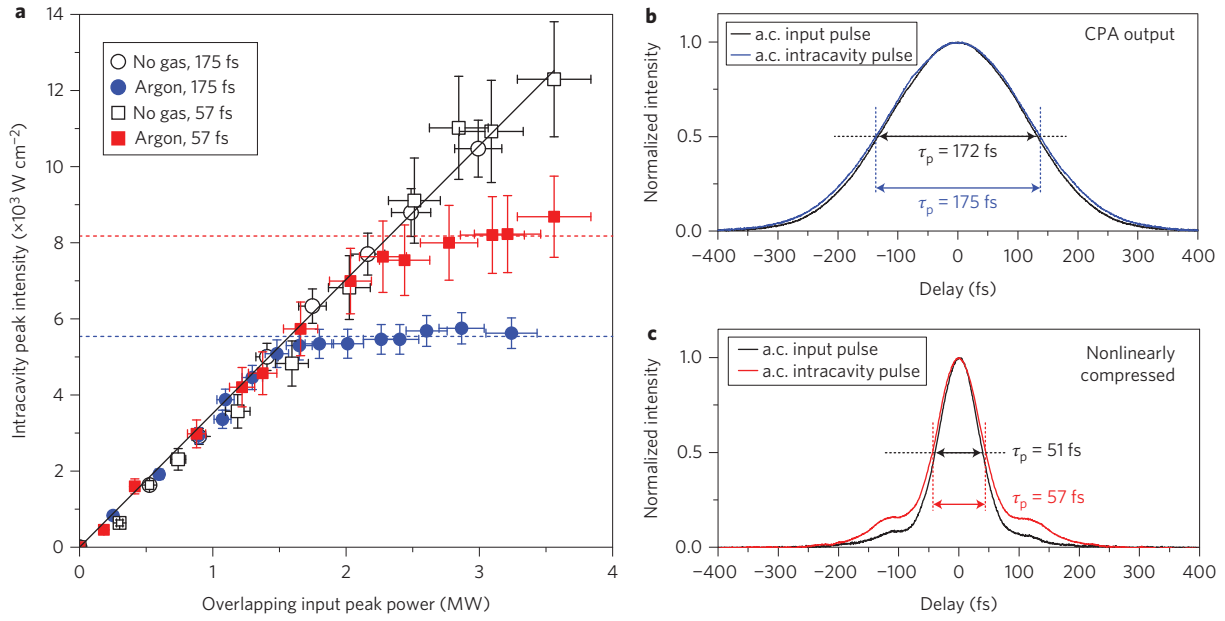

Figure 3 | Intensity upper bound for uncompressed and nonlinearly compressed pulses. a, Peak intensity at the $w_0 = 20$ μm focus as a function of the input peak power coupled to the cavity fundamental mode. The latter is obtained from the peak power of the laser by consideration of the spatial and spectral overlap with the fundamental mode of the empty cavity. In the absence of a gas target, the dependence is linear, with the same slope for uncompressed (175 fs) and compressed (57 fs) pulses. With argon injected at the focus, a clamping of the peak intensity is observed at high power levels. The dashed lines indicate intensity clamping levels, showing that the compressed pulses allow for considerably higher intensities. Error bars indicate the systematic measurement uncertainty. **b**,**c**, Intensity autocorrelation traces of the pulses from the chirped-pulse amplifier (CPA, **b**) and of the nonlinearly compressed pulses (**c**).

energy (Fig. 2d). Although this output coupling method is conceptually simple[22], the realization of an appropriate pierced mirror is technologically challenging. First, a clear aperture of several tens of micrometres is necessary for coupling out the XUV radiation. Moreover, the surface surrounding the aperture needs to remain unaffected by the drilling process to minimize the cavity losses for the fundamental radiation (see Methods).

The effect of the hole on the resonant transverse mode can be understood by means of a coherent mode coupling model[26]. This predicts that fundamental-mode operation can be achieved with a roundtrip loss factor of $1 - \exp[-4(r_h/w)^2]$, where r_h is the hole radius and w is the spot size on the mirror ($1/e^2$ radius of the intensity). For our parameters ($r_h \approx 80$ μm, $w \approx 2.7$ mm) a power enhancement of up to 250 is experimentally reached without a gas target, which is in good agreement with the model. The power enhancement is diminished by 38% when compressed pulses are used, mainly due to imperfect spectral overlap of the laser comb modes with the cavity resonances. The excellent Gaussian fit to the measured intensity profile at the mirror preceding the cavity focus (Fig. 2e) confirms the expected fundamental-mode operation. With uncompressed input pulses, the circulating power in the empty cavity is limited to 8 kW by nonlinear effects in the mirrors[24]. With compressed pulses, a slow drift on the timescale of a minute of the free-running second comb parameter is manually compensated by displacing a pair of wedges inside the oscillator[1].

Our first experiment addressed the pulse-duration dependence of the limitations introduced by ionization in the gas target. It has been observed previously that this effect causes a clamping of the circulating power[18,20,21]. Because the decay time of the plasma generated in the focus is considerably longer than the repetition period of the pulses, a steady-state ionization is induced, which makes locking of the laser to the cavity more difficult[20]. More harmful is the ionization during the pulse, which generates a dynamic frequency change. As a result, a phase shift is accumulated during the pulse. At the end of the pulse the phase change is given by[21]

$$\varphi_p = k\frac{L}{2n_{cr}} \times (n_p - n_{ss}) \quad (1)$$

where k is the wavenumber of the radiation, L is the length of the plasma, n_{cr} is the critical electron density (at which the plasma frequency equals the laser frequency) and n_p and n_{ss} are the electron density at the end of the pulse and the steady-state electron density, respectively. Equation (1) is valid if both n_p and n_{ss} are much smaller than the critical electron density. A significant reduction of the enhancement factor provided by the cavity is expected if $\varphi_p > \pi/F$, where F is the cavity finesse[19]. The intensity in the focus will thus be clamped at values generating phase shifts of this magnitude. In the spectral domain, the frequency change during the pulse manifests itself as a blueshift, which reduces the overlap between the seed pulse and the pulse circulating in the cavity. An obvious way to solve this problem is to reduce the cavity finesse, but this requires a corresponding increase in the power delivered by the driving laser system[18]. A more efficient method is to reduce the pulse duration; keeping the intensity constant, n_p decreases approximately in proportion with the pulse duration. In contrast, for a weakly ionized plasma whose decay is dominated by three-body recombination, n_{ss} decreases only with the third root of the pulse duration. Therefore, the term in brackets in equation (1) diminishes rapidly with decreasing pulse duration, so clamping of the intensity due to plasma effects can be overcome by using shorter pulses. To confirm this expectation, we increased the input power to the cavity for uncompressed and nonlinearly compressed pulses and recorded the intracavity peak intensity by using argon gas as the nonlinear medium and a beam waist radius of $w_0 = 20$ μm. Indeed, the measured clamping level of the peak intensity was found to increase significantly when using compressed

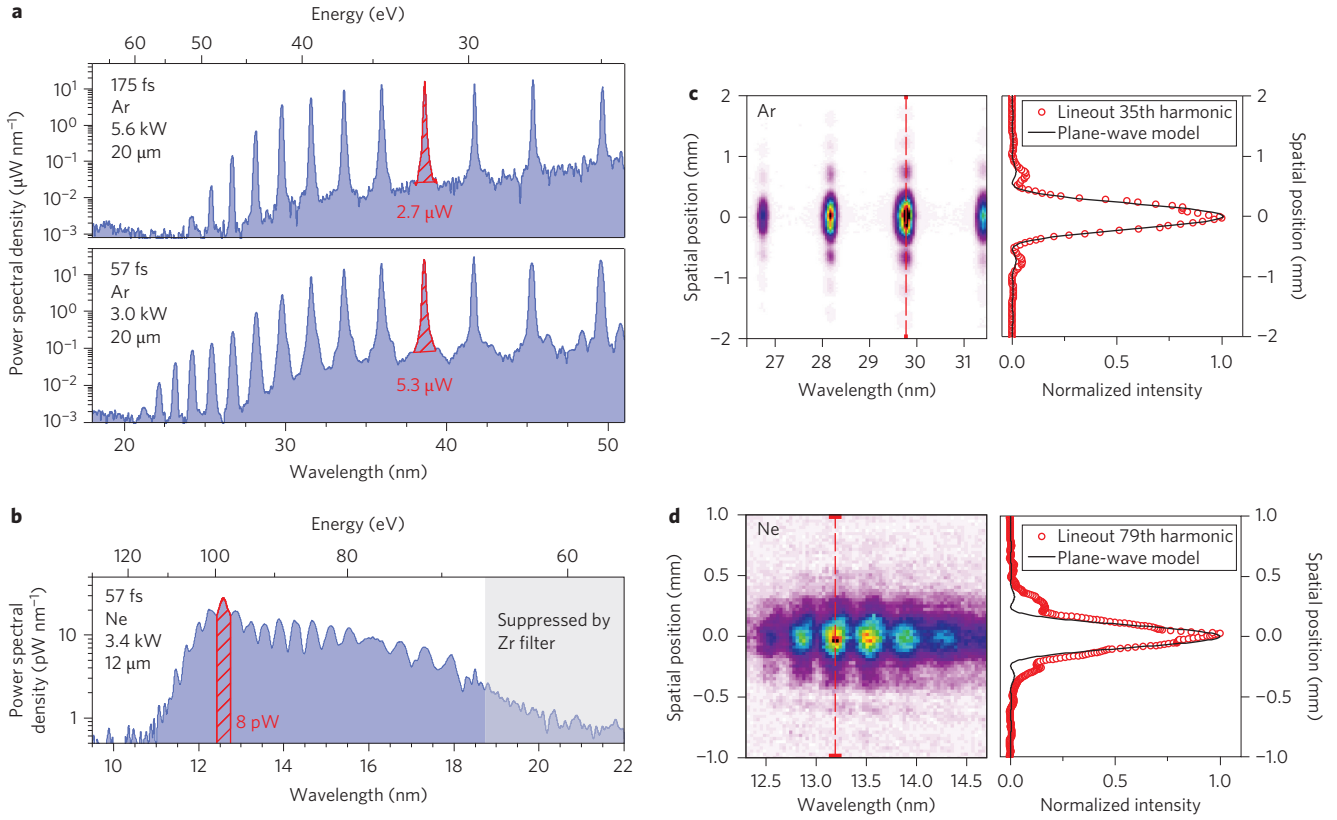

Figure 4 | Harmonic spectra and beam profiles. a, Spectra generated in argon with uncompressed ('CPA output') and nonlinearly compressed pulses for $w_0 = 20$ µm. All values refer to the output coupled radiation behind the pierced mirror. **b**, Spectrum generated in neon with compressed pulses and a tighter focus with $w_0 = 12$ µm. **c**,**d**, XUV beam profiles and corresponding lineouts of harmonics generated in argon (**c**) and neon (**d**). For lower-order harmonics (here 35th), the transverse profile of the XUV beam inside the cavity is substantially larger than the clear aperture of the hole, leading to an Airy diffraction pattern in the far field. The solid black line indicates the diffraction pattern expected at the detector for the diffraction of a plane wave at the pierced mirror. For higher orders (here 79th), the far-field distribution deviates substantially from the plane-wave model, confirming the decreasing XUV beam divergence.

pulses (Fig. 3), corroborating that shorter pulses mitigate ionization-related enhancement limitations.

The spectra and spatial profiles of the generated XUV radiation (Fig. 4) were monitored with a grazing-incidence spectrometer, and the power of the 27th harmonic was measured with a calibrated XUV photodiode after dispersing the output coupled harmonics with a grating (see Methods). Stable locking was achieved with both uncompressed and compressed pulses, with a relative root-mean square of the intracavity intensity fluctuations lower than 0.5% in the range between 250 Hz and 1 MHz. We detected microwatt-level harmonics down to wavelengths below 30 nm (Fig. 4a). This power level approaches the values demonstrated with the brightest state-of-the-art low-repetition-rate sources[11]. The use of nonlinearly compressed pulses leads to a significant increase in the XUV average power and in the generated XUV photon energies.

To demonstrate the scalability of our concept towards the soft X-ray region, we used tighter focusing ($w_0 = 12$ µm) and neon as a nonlinear medium (because of its high ionization potential). Harmonics up to order 91, corresponding to 11.45 nm or 108 eV, were detected (Fig. 4b), surpassing the highest previously generated photon energies at similar repetition rates[4,12,13,19,27] by a factor of almost 4. The measured harmonic power with neon steadily increased with the backing pressure in the gas nozzle; however, this pressure was limited to 1 bar by the capacity of our turbomolecular vacuum pump.

In conclusion, we have overcome the previous limitations of cavity-enhanced HHG by implementing two major improvements. First, we enhanced nonlinearly compressed pulses generated by an Yb-based laser. This provides a unique combination of short pulse durations and high average powers, mitigating ionization-related effects and thus allowing for a scaling of the generated photon energies. Second, we coupled out the generated radiation through a pierced mirror, experimentally applying this method for high harmonics for the first time. Our experiments demonstrate the feasibility of extending this technique towards the generation of soft X-rays and identify a straightforward strategy for scaling cavity-enhanced HHG towards both higher XUV photon energies and photon flux. To this end, higher input powers delivered by state-of-the-art lasers[27] can be coupled to enhancement cavities with optimized designs with larger spot sizes on the mirrors. The XUV radiation generated with such a source lends itself to a multitude of applications in science and technology[11,28]. In particular, the versatility of geometric output coupling promises the applicability of gating techniques[10] for confining HHG to a single cycle of the intracavity field. Thus, the generation of isolated attosecond pulses at megahertz repetition rates is within reach, paving the way for high-repetition-rate attosecond metrology. Moreover, increasing the photon flux around 13 nm with a compact source will have a significant impact on next-generation semiconductor technology[5].

Methods

Experimental parameters. Nonlinear compression after chirped-pulse amplification was achieved by spectral broadening in a large-mode-area fibre (mode-field diameter, 59 µm; length, 2.6 cm) followed by chirped mirrors with a total group delay dispersion of −2,600 fs^2. The focusing arrangement of the cavity was asymmetric, with two curved mirrors. The experiments were performed with a looser focus ($w_0 = 20$ µm), with radii of curvature of 100 and 300 mm, or with a tighter focus ($w_0 = 12$ µm), with radii of 38 and 150 mm, respectively. Gas was injected at the focus through an end-fire glass nozzle with an inner diameter of

100 μm. The gas target position and backing pressure (2.5 bar for argon) were chosen empirically to maximize the output coupled power of the 27th harmonic. The pulse duration τ_p was calculated by assuming a sech^2 temporal intensity envelope. The autocorrelation of the compressed pulses exhibited a pedestal (~10% of total power) that was accentuated upon enhancement in the cavity (~20% of total power), indicating the limited optical bandwidth of the cavity.

The output coupling efficiency could be estimated by invoking a strong field model in which the dipole moment varies with the power p of the fundamental laser field, with $p < q$, where q is the harmonic order[29]. For plateau harmonics $p \approx 5$ has been found to be an appropriate choice[29]. We approximated the beam divergence of the qth harmonic by $\theta_p = (\lambda\sqrt{p}/\pi w_0 q)$ where λ denotes the wavelength of the fundamental radiation and w_0 the beam waist radius. The spot size of the harmonic beam at the output coupling mirror is given by $w = d\theta_q$, where d is the distance between the focus and the mirror. Radial integration then results in an output coupling efficiency given by $T_q = 1 - \exp[-2(r_{hc}/w)^2]$, where r_{hc} denotes the clear aperture radius.

Hole manufacturing and effect on the transverse mode. The hole on the mirror surface, continuing in a conical notch towards the back side of the substrate, was manufactured by inverse laser drilling into a fused-silica mirror substrate before the coating process. The beam of a diode-seeded regenerative amplifier with a pulse energy of 250 μJ at a repetition rate of 10 kHz, wavelength of 1,064 nm and pulse duration around 1 ns was focused through the bulk onto the bottom surface and scanned laterally. The cone-shaped opening was drilled layer by layer. The transverse distortion introduced by the hole to the intracavity field led to coherent coupling of the fundamental mode to higher-order transverse modes[26]. The resulting field distribution could be decomposed in terms of Hermite–Gaussian eigenmodes of the cavity without the hole, and the coefficients of this decomposition depend on the aperture function $t(x,y)$ as well as on the diffraction losses and on the relative phase of the respective modes. If the transverse dimension of the distortion is small compared to the extent of the field $E(x,y)$ impinging on the pierced mirror, many modes of high orders with small-magnitude coefficients are necessary for the decomposition[26]. Consequently, a large number of these modes are suppressed by the finite size of the cavity mirrors. Therefore, the contribution of higher-order modes to the circulating field can be neglected and the field distribution $E(x,y)$ impinging on the pierced mirror is well approximated by the fundamental mode of the cavity without the hole. The total power coupled by this mirror into the non-resonant higher-order modes is proportional to the $x - y$ integral over $|[1 - t(x,y)]E(x,y)|^2$, and the power attenuation of the fundamental mode $E(x,y)$ due to geometric transmission losses upon reflection at this mirror is given by the same factor. For a Gaussian beam with radius w and a circular hole with radius r_h this implies overall roundtrip losses of $1 - \exp[-4(r_h/w)^2]$.

XUV detection and power measurement. The harmonic radiation was monitored with a grazing-incidence spectrometer equipped with a concave grating (600 grooves mm^{-1}). The spectrally resolved intensity distribution was recorded with a charge-coupled device (CCD) camera placed at the Rowland circle. The relative output coupled XUV spectral intensity was calculated from the CCD camera signal, considering the overall detection efficiency. The increasing noise floor towards longer wavelengths was due to the decreasing detection efficiency. For the argon experiments the power spectral density was obtained with an additional absolute power measurement, performed by angularly dispersing the output coupled radiation with a calibrated fused silica grating (1,960 grooves mm^{-1}) and by measuring the power of the 27th harmonic with an Al-coated XUV photodiode (IRD AXUV100Al3). For the neon measurement, the gas target parameters were chosen to optimize phase matching for the cutoff region, resulting in powers too low for a measurement with the XUV photodiode in its sensitive spectral range. The power spectral density in Fig. 4b is therefore a rough estimate obtained from the spectrometer measurement and can be considered as a lower bound for the actual power.

Received 26 March 2013; accepted 22 May 2013; published online 7 July 2013

References

1. Gohle, C. *et al.* A frequency comb in the extreme ultraviolet. *Nature* **436,** 234–237 (2005).
2. Jones, R. J., Moll, K. D., Thorpe, M. J. & Ye, J. Coherent frequency combs in the vacuum ultraviolet via high-harmonic generation inside a femtosecond enhancement cavity. *Phys. Rev. Lett.* **94,** 193201 (2005).
3. Hartl, I. *et al.* Cavity-enhanced similariton Yb-fiber laser frequency comb: 3×10^{14} W/cm^2 peak intensity at 136 MHz. *Opt. Lett.* **32,** 2870–2872 (2007).
4. Cingöz, A. *et al.* Direct frequency comb spectroscopy in the extreme ultraviolet. *Nature* **482,** 68–71 (2012).
5. Stolow, A., Bragg, A. E. & Neumark, D. M. Femtosecond time-resolved photo electron spectroscopy. *Chem. Rev.* **104,** 1719–1757 (2004).
6. Zhang, C-H. & Thumm, U. Attosecond photoelectron spectroscopy of metal surfaces. *Phys. Rev. Lett.* **102,** 123601 (2009).
7. Lin, J. *et al.* At-wavelength inspection of sub-40 nm defects in extreme ultraviolet lithography mask blank by photoemission electron microscopy. *Opt. Lett.* **32,** 1875–1877 (2007).
8. Krausz, F. & Ivanov, M. Attosecond physics. *Rev. Mod. Phys.* **81,** 163–234 (2009).
9. Hentschel M. *et al.* Attosecond metrology. *Nature* **414,** 509–513 (2001).
10. Sansone, G., Poletto, L. & Nisoli, M. High-energy attosecond light sources. *Nature Photon.* **5,** 655–663 (2011).
11. Mills, A., Hammond, T. J., Lam, M. H. C. & Jones, D. J. XUV frequency combs via femtosecond enhancement cavities. *J. Phys. B* **45,** 142001 (2012).
12. Park, I-Y. *et al.* Plasmonic generation of ultrashort extreme-ultraviolet light pulses. *Nature* **5,** 677–681 (2011).
13. Vernaleken, A. *et al.* Single-pass high-harmonic generation at 20.8 MHz repetition rate. *Opt. Lett.* **36,** 3428–3430 (2011).
14. Stockman, M., Kling, M. F., Kleineberg, U. & Krausz, F. Attosecond nanoplasmonic-field microscope. *Nature Photon.* **1,** 539–544 (2007).
15. Chew, S. H. *et al.* Time-of-flight-photoelectron emission microscopy on plasmonic structures using attosecond extreme ultraviolet pulses. *Appl. Phys. Lett.* **100,** 051904 (2012).
16. Sansone, G. *et al.* Electron localization following attosecond molecular photoionization. *Nature* **465,** 763–766 (2010).
17. Bergues, B. *et al.* Attosecond tracing of correlated electron-emission in non-sequential double ionization. *Nat. Commun.* **3,** 813 (2012).
18. Yost, D. *et al.* Power optimization of XUV frequency combs for spectroscopy applications [Invited]. *Opt. Express* **19,** 23483–23493 (2011).
19. Lee, J., Carlson, D. R. & Jones, R. J. Optimizing intracavity high harmonic generation for XUV fs frequency combs. *Opt. Express* **19,** 23315–23326 (2011).
20. Carlson, D. R., Lee, J., Mongelli, J., Wright, E. M. & Jones, R. J. Intracavity ionization and pulse formation in femtosecond enhancement cavities. *Opt. Lett.* **36,** 2991–2993 (2011).
21. Allison, T. K., Cingöz, A., Yost, D. C. & Ye, J. Extreme nonlinear optics in a femtosecond enhancement cavity. *Phys. Rev. Lett.* **107,** 183903 (2011).
22. Moll, K. D., Jones, R. J. & Ye, J. Output coupling methods for cavity based high-harmonic generation. *Opt. Express* **14,** 8189–8197 (2006).
23. Eidam, T., Röser, F., Schmidt, O., Limpert, J. & Tünnermann, A. 57 W, 27 fs pulses from a fiber laser system using nonlinear compression. *Appl. Phys. B* **92,** 9–12 (2008).
24. Pupeza, I. *et al.* Power scaling of a high-repetition-rate enhancement cavity. *Opt. Lett.* **35,** 2052–2054 (2010).
25. Jocher, C., Eidam, T., Hädrich, S., Limpert, J. & Tünnermann, A. Sub 25 fs pulses from solid core nonlinear compression stage at 250 W of average power. *Opt. Lett.* **37,** 4407–4410 (2012).
26. Paschotta, R. Beam quality deterioration of lasers caused by intracavity beam distortions. *Opt. Express* **14,** 6069–6074 (2006).
27. Hädrich, S. *et al.* Generation of μW level plateau harmonics at high repetition rate. *Opt. Express* **19,** 19374–19383 (2011).
28. Jaegle, P. *Coherent Sources of XUV Radiation* (Springer, 2006).
29. L'Huillier, A., Balcou, P., Candel S., Schafer, K. J. & Kulander, K. C. Calculations of high-order harmonic-generation processes in xenon at 1064 nm. *Phys. Rev. A* **46,** 2778–2790 (1992).
30. Drever, R. W. P. *et al.* Laser phase and frequency stabilization using an optical resonator. *Appl. Phys. B* **31,** 97–105 (1983).

Acknowledgements

This work was supported by the Deutsche Forschungsgemeinschaft (DFG) Cluster of Excellence, Munich Centre for Advanced Photonics (MAP) (www.munich-photonics.de), by the KORONA Max-Planck-Institut für Quantenoptik (MPQ)/Fraunhofer-Institut für Lasertechnik (ILT) cooperation and by the Bundesministerium für Bildung und Forschung (BMBF) under PhoNa – Photonische Nanomaterialien (contract no. 03IS2101B).

Author contributions

The project was planned by I.P., S.H., J.R., J.L., T.U., A.T., T.W.H., A.A., F.K. and E.F. The Yb:fibre laser was designed and built by T.E., J.L. and A.T. The piercing in the substrate for the XUV output coupling mirror was realized by D.E., J.W. and P.R. The HHG experiments and model development were performed by I.P., S.H., T.E., H.C., J.W. and E.F. All authors discussed the results and contributed to the final manuscript.

Additional information

Reprints and permissions information is available online at www.nature.com/reprints. Correspondence and requests for materials should be addressed to I.P.

Competing financial interests

The authors declare no competing financial interests.